

Device Characteristics with Potential Fluctuation Induced by Nonuniformity at Gate Oxide Interface with Multifractal Analysis

Yoshio Ashizawa, Ryo Tanabe and Hideki Oka
 Fujitsu Laboratories Ltd.
 50 Fuchigami, Akiruno, Tokyo, 197-0833, Japan
 E-mail: ashizawa.yoshio@jp.fujitsu.com

Abstract—Nonuniformity at the gate oxide interface is considered to be one of the serious fluctuation issues, which is induced by polysilicon grain boundary, impurity segregation, silicide and high-k stack. We introduce a mosaic layer at the gate oxide interface and relate the degree of the nonuniformity with device characteristics through multifractal analysis. There is an analogy between the degree of randomness and thermodynamics. More entropy increase in the mixture gives less variation in device characteristics. Finally, we discuss the allowable nonuniformity which is caused by unintended process variation in the view of pattern.

Keywords—component; nonuniformity; polysilicon gate; grain boundary; high-k stack; multifractal

I. INTRODUCTION

Device characteristics fluctuation induced by random dopant in the channel and poly-Si gate [1] [2] has been investigated. However, simulated variations are still less than experimental data. Nowadays it is reported that the nonuniformity [3] [4] at the gate oxide interface can be comparable source to random dopant fluctuation in the substrate. Therefore, we demonstrate that local potential fluctuation at the gate surface affects device characteristics by placing a thin mosaic layer at the interface. Moreover, we introduce multifractal technique to relate the randomness of the pattern with device characteristics. This image processing idea can be applicable to evaluating process without measuring electrical device characteristics.

II. DEVICE STRUCTURE AND MODELING

A. Mosaic Pattern Layer at the Gate Oxide Interface

Fig. 1 shows schematic device structure and parameters. While doping profile is given analytically, a mosaic tile layer is introduced at the poly-Si interface. There are 500 mosaic tiles. A random number ranging from 0 to 1 is given to each tile. And the value is mapped to either high (10^{20}cm^{-3}) or low (10^{19}cm^{-3}) doping concentration by comparing the given random number with some cut-off parameter p_c or high coverage ratio, which is also ranging from 0 to 1. In the end, the work function of gate surface is locally fluctuated by the mosaic pattern.

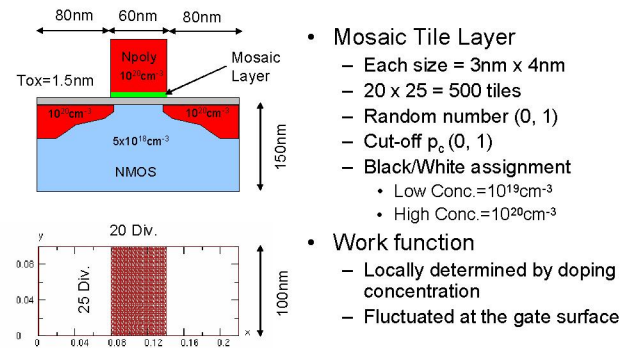


Figure 1. Device structure and parameters for simulation.

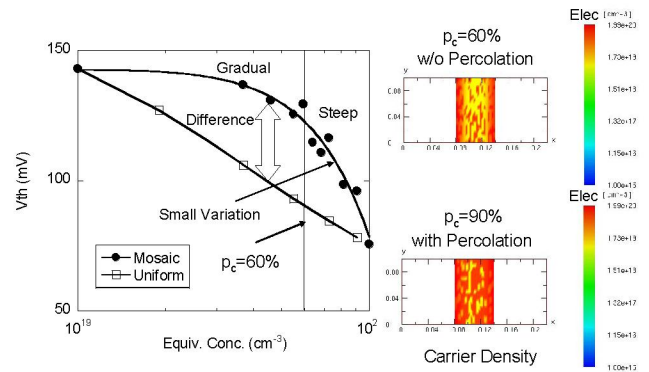


Figure 2. Equivalent concentration vs. V_{th} (left) and electron distribution between $p_c=60\%$ and 90% (right).

Fig. 2 shows the V_{th} distribution for equivalent concentration, which is calculated by averaging over the doping concentration at the gate surface. V_{th} varies gradually with low concentration but it decreases steeply at high concentration.

In the 2D mosaic pattern shown in Fig. 3, the electrical conduction is generally characterized by the cut-off parameter p_c . The electrical property is dramatically changed around $p_c=60\%$ due to the percolation, which establishes the current path along the high value pattern between both sides. It is

observed that current path is established for $p_c=90\%$ in contrast to $p_c=60\%$ in Fig. 2.

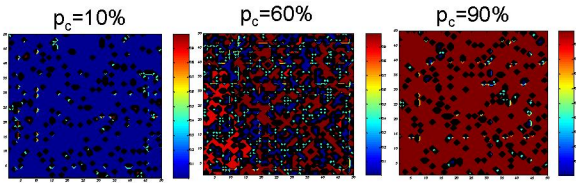


Figure 3. 2D random mosaic pattern with varying cut-off parameter p_c .

This suggests that the gate surface be modeled in mosaic pattern because large difference is observed between mosaic pattern and conventional continuous doping. But it is interesting that V_{th} plots for mosaic pattern are almost on the curve in Fig. 2. This implies that uniformly random mosaic pattern gives small variation.

B. Generation of Nonuniform Patterns

Fig. 4 shows the simulation procedure to generate nonuniform pattern, which is based on Brownian dynamics. The pattern is determined by the competition between diffusion and random noise statistically.

Stochastic Equation (Brownian Dynamics)

$$\frac{\partial h(x, y, t)}{\partial t} = A \eta(x, y, t) + D \left(\frac{\partial^2}{\partial x^2} + \frac{\partial^2}{\partial y^2} \right) h(x, y, t)$$

Noise Diffusion

- I.C.: Uniform Random Number
- B.C.: Periodical Boundary Condition

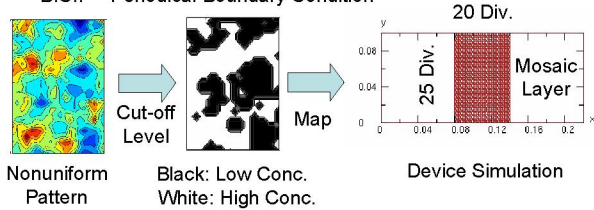


Figure 4. Generation of nonuniform pattern.

Fig. 5 shows the growing nonuniform pattern from initial random pattern, where grain size is adjusted around 20 nm.

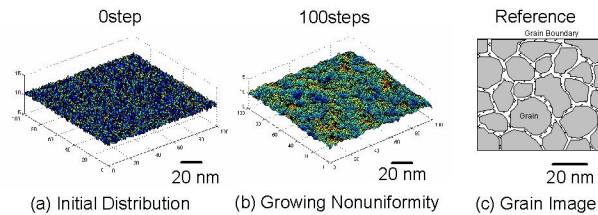


Figure 5. Growing nonuniform pattern with Brownian dynamics.

III. MULTIFRACTAL ANALYSIS

Multifractal analysis technique is introduced to characterize randomness of the complicated patterns. The conventional fractal dimension tells us how the length, area or density of an object varies with scaling. But much more information is required to characterize or model the more complicated

structures that occur in nature. The major efforts in multifractal objects have been directed toward the understanding of subset of the more complicated fractal objects. Box count dimension technique is applied to calculate generalized dimensions [5].

Fig. 6 explains the calculation procedure for generalized dimension $D(q)$, which represents spatial structure characterized by moment q . The singular spectrum $f(\alpha)$ is defined by the Legendre transformation of mass exponent $\tau(q)$, i.e., $f(\alpha)=q\alpha-\tau(q)$, where α means the Lipschitz-Hölder exponent. The singular spectrum $f(\alpha)$ is fractal dimension for spatial distribution of boxes characterized by the exponent α , where α can be also calculated directly from box count slope of wave function amplitude $Z(q)$.

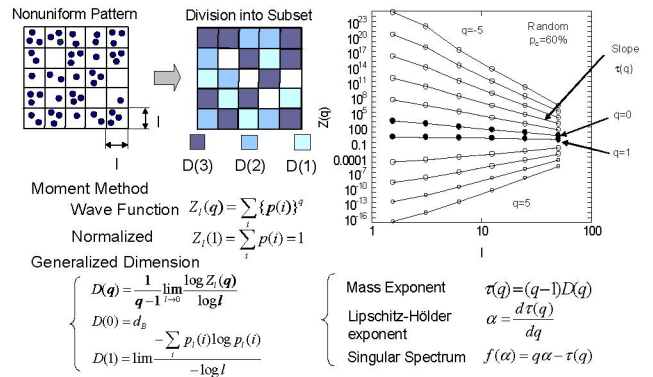


Figure 6. Calculation procedure for generalized dimension.

The moment q is analogous to inverse temperature $1/T$ in the N particle system except that q can be a negative value. The variation principle for $\tau(q)$ is analogous to $\Delta F = \Delta E - T\Delta S$, where $\tau(q)$ corresponds to free energy $\Delta F/T$, $f(\alpha)$ to entropy ΔS and α to internal energy $\Delta E/T$ respectively in Fig. 7. This analogy to the thermodynamics helps understanding the meanings of these dimensionless variables.

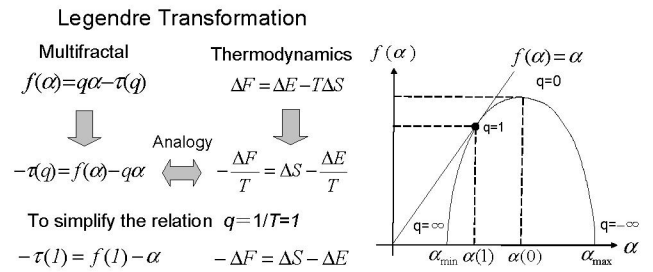


Figure 7. Analogy of multifractal to thermodynamics.

IV. SINGULAR SPECTRA FOR RANDOM PATTERN

Fig 8 shows the $f(\alpha)$ spectra for uniformly random patterns. The percentages correspond to cut-off parameters p_c ranging from 10 to 99 %. Each $f(\alpha)$ spectrum has a contact point at $q=1$ on the line $f(\alpha)=\alpha$, where the free energy is zero, $-\tau(1)=f(\alpha)-\alpha=0$. This special $f(\alpha)$ is known as the information dimension. The tracks of the information dimension lie on $f(\alpha)=\alpha$.

We focus on the spectra for positive q here because they characterize the distribution for high concentration mosaic tiles, which gives lower threshold voltage. The spectra range represents the degree of entropy in the mixture. It goes down as increasing q . Wide range of spectra means that the pattern is more uniform like white noise because it has various component of moment q .

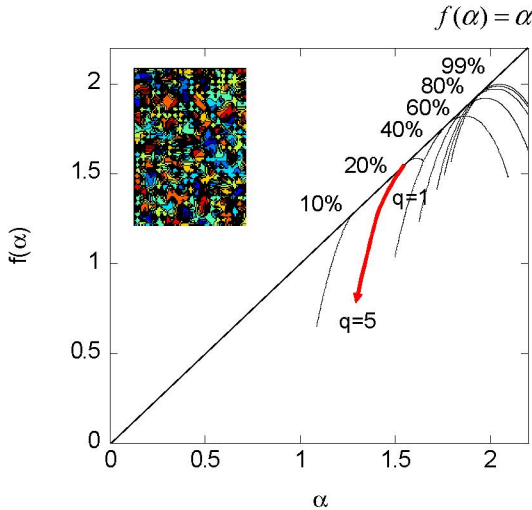


Figure 8. $f(\alpha)$ spectra for uniformly random patterns.

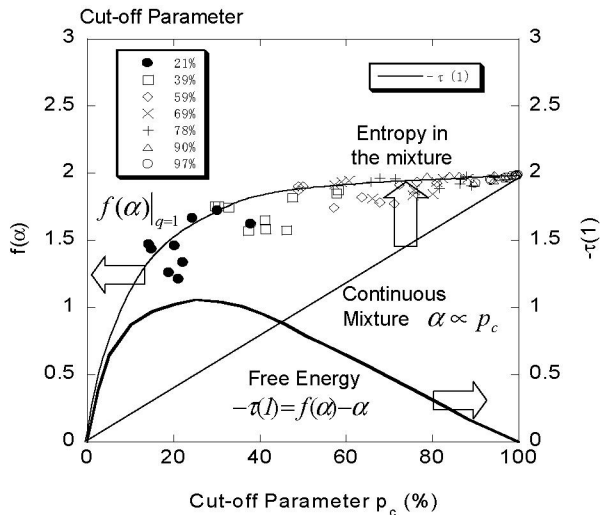


Figure 9. Singular spectra $f(\alpha)$ and mass exponent $-\tau(q)$ as a function of p_c .

Fig. 9 shows the relation between $f(\alpha)$ and $-\tau(1)$ as a function of p_c . We are particularly interested in $-\tau(1)$ because it simplifies the calculation of each term especially to let $q=1/T=1$. The $f(\alpha)$ spectra for uniformly random patterns are plotted with cut-off parameters, where $f(\alpha)=0$ at $p_c=0\%$ and $f(\alpha)=2$ at $p_c=100\%$. The internal energy α for continuous mixture is linearly distributed between both ends as well as the average concentration over the layer is calculated by the cut-off parameter. The free energy $-\tau(1)$ by the increase of entropy in the mixture is calculated by the simple relation $f(\alpha)-\alpha$ at $q=1$.

It takes a peak around 30%. This is the characteristics for 2D random mosaic pattern.

V. SINGULAR SPECTRA FOR NONUNIFORM PATTERN

Fig. 10 shows the $f(\alpha)$ spectra for nonuniform patterns. The difference from uniform pattern is that spectra lose the range of $f(\alpha)$ with decreasing p_c . The $f(\alpha)$ spectrum at $p_c=20\%$ converges to a point. We are interested in this ranging difference with varying q and discuss in the next session.

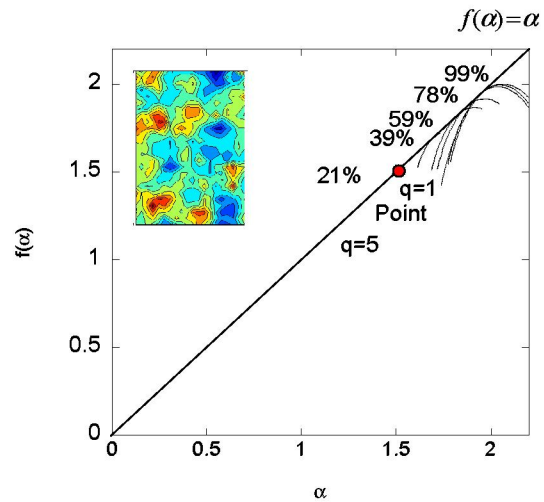


Figure 10. $f(\alpha)$ spectra for nonuniform patterns.

VI. NONUNIFORMITY AND DEVICE CHARACTERISTICS

Fig. 11 shows the relation between ΔV_{th} and $\Delta f(\alpha)$ for nonuniform patterns, where V_{th} is defined as the deviation from that of uniformly random pattern and $\Delta f(\alpha)$ is calculated by the range of $f(\alpha)$ with varying q between 1 and infinity. The deviation ΔV_{th} only represents the effect of mosaic patterns because the operation above subtracts the threshold voltage change due to percolation.

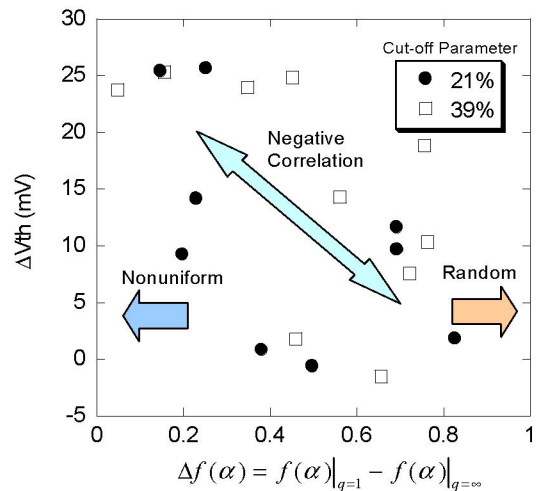


Figure 11. Relationship between ΔV_{th} and $\Delta f(\alpha)$ for nonuniform patterns.

It is found that ΔV_{th} is negatively correlated with $\Delta f(\alpha)$. Larger $\Delta f(\alpha)$ gives smaller deviation ΔV_{th} because larger $\Delta f(\alpha)$ means more stable by increase of entropy in the mixture.

Fig. 12 shows the deviation ΔV_{th} for each nonuniform pattern and $-\tau(I)$ for uniformly random pattern. As for uniformly random pattern, all of ΔV_{th} plots are on the convex curve $-\tau(I)$ as shown in Fig. 9. As for nonuniform pattern, most of them for higher p_c are on the curve $-\tau(I)$. But they are out of the curve for lower p_c . If the pattern is nearly uniformly random, ΔV_{th} approaches to the convex curve $-\tau(I)$. However, if the pattern has nonuniformity, ΔV_{th} shows some smaller value than $-\tau(I)$. The difference between the plot and the curve represents the degree of nonuniformity.

It is preferable against device characteristics fluctuation to apply the process with higher p_c nonuniformity if the process has unintended variation.

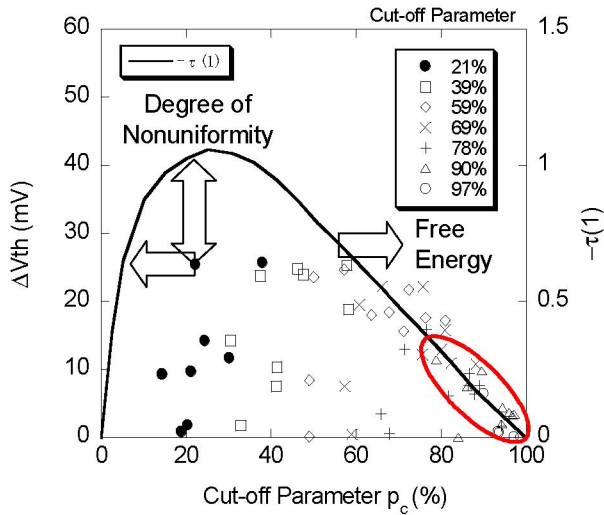


Figure 12. Relationship between ΔV_{th} and p_c with $-\tau(q)$.

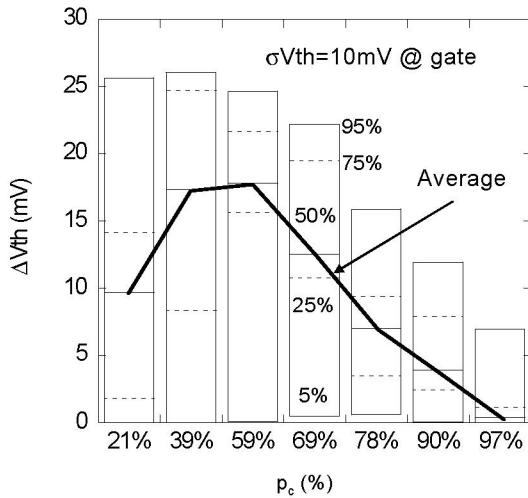


Figure 13. Frequency of ΔV_{th} as a function of average cut-pff parameter.

Fig. 13 shows the ΔV_{th} distribution for nonuniform patterns as a function of cut-off parameter p_c . The percentages in the bar represent cumulative ΔV_{th} distribution. The average line represents the mean value within each distribution bar. Large ΔV_{th} is observed at lower p_c around 30 %. The range distribution is similar to the curve $-\tau(I)$ in Fig. 12.

The average σV_{th} for all coverage ratios is 10 mV. This is not negligible against 20 mV σV_{th} for random dopant fluctuation in the substrate for this structure.

It is very helpful to apply multifractal technique to relate the process nonuniformity with device characteristics. And it gives quantitative evaluation of the nonuniformity that has been considered to be “random”.

VII. CONCLUSION

We have evaluated device characteristics fluctuation by placing a mosaic layer at the gate oxide interface, which has not been considered quantitatively.

The interface should be modeled in mosaic pattern for nonuniform materials, such as polysilicon, silicide and high-k stack. We introduce multifractal technique and relate the nonuniformity with device characteristics. More increase of entropy of the mosaic mixture gives less variation in device characteristics. Moreover, the impact of nonuniformity to device characteristics fluctuation is not negligible against that of random dopant in the substrate.

This result suggests that ΔV_{th} be the outcome of nonuniformity at the gate oxide interface. It is preferable against device characteristics fluctuation to apply the process with higher p_c nonuniformity in the view of pattern dynamics.

REFERENCES

- [1] A. Asenov and S. Saini, “Polysilicon gate enhancement of the random dopant induced threshold voltage fluctuations in sub-100 nm MOSFETs with ultrathin gate oxide,” IEEE Trans. Electron Devices, 47, pp. 805-812, 2000.
- [2] S. Shimizu, T. Kuroi, H. Sayama, A. Furukawa, Y. Nishida, Y. Inoue, M. Inuishi and T. Nishimura, “Gate electrode engineering by control of grain growth for high performance and high reliable 0.18μm CMOS,” VLSI Tech. Dig., pp. 107-108, 1997
- [3] A. R. Brown, J. R. Watling, A. Asenov, G. Bersuker and P. Zeitloff, “Intrinsic parameter fluctuations in MOSFETs due to structural non-uniformity of high-k gate stack materials,” SISPAD 2005, pp.27-30.
- [4] H. Watanabe, “Statistics of grain boundaries in gate poly-Si,” SISPAD 2005, pp. 39-42.
- [5] T. C. Halsey, M. H. Jensen, L. P. Kadanoff, I. Procaccia and B. I. Shraiman, “Fractal measures and their singularities: the characterization of strange sets,” Phys. Rev. A 33, pp. 1141-1151.